An AlGaN/GaN HEMT with a reduced surface electric field and an improved breakdown voltage

Xie Gang(谢 刚)[a)b)†], Edward Xu[a)], Niloufar Hashemi[a)],
Zhang Bo(张 波)[b)], Fred Y. Fu[c)], and Wai Tung Ng[a)]

[a)] *The Edward S. Rogers Sr. Electrical and Computer Engineering Department, University of Toronto, Toronto, Ontario M5S 1A1, Canada*

[b)] *State key Laboratory of Electronic Thin Films and Integrated Devices, University of Electronic Science and Technology of China, Chengdu* 610054, *China*

[c)] *Crosslight Software Inc. Burnaby, BC, Canada*

(Received 15 December 2011; revised manuscript received 14 February 2012)

A reduced surface electric field in an AlGaN/GaN high electron mobility transistor (HEMT) is investigated by employing a localized Mg-doped layer under the two-dimensional electron gas (2-DEG) channel as an electric field shaping layer. The electric field strength around the gate edge is effectively relieved and the surface electric field is distributed evenly as compared with those of HEMTs with conventional source-connected field plate and double field plate structures with the same device physical dimensions. Compared with the HEMTs with conventional source-connected field plates and double field plates, the HEMT with a Mg-doped layer also shows that the breakdown location shifts from the surface of the gate edge to the bulk Mg-doped layer edge. By optimizing both the length of Mg-doped layer, $L_{\rm m}$, and the doping concentration, a 5.5 times and 3 times the reduction in the peak electric field near the drain side gate edge is observed as compared with those of the HEMTs with source-connected field plate structure and double field plate structure, respectively. In a device with $V_{\rm GS} = -5$ V, $L_{\rm m} = 1.5$ μm, a peak Mg doping concentration of 8×10^{17} cm^{-3} and a drift region length of 10 μm, the breakdown voltage is observed to increase from 560 V in a conventional device without field plate structure to over 900 V without any area overhead penalty.

Keywords: AlGaN/GaN HEMT, reduced surface electric field, Mg-doped layer, breakdown voltage

PACS: 61.72.uj, 71.20.N, 51.50.+v **DOI:** 10.1088/1674-1056/21/8/086105

1. Introduction

The AlGaN/GaN high electron mobility transistor (HEMT) is a promising candidate for microwave and high voltage applications due to its wide band gap, two-dimensional electron gas, high saturation velocity, and low intrinsic carrier density.[1−4] In order to fully develop the potential of HEMTs and suppress the current collapse effect, it is important to suppress the drain side gate edge electric field strength.[5,6] Field plate (FP) structures have been shown to be effective in enhancing the breakdown voltage and suppressing the drain side gate edge electric field strength.[7] In addition, an FP can improve device reliability and suppress current collapse from occurring in AlGaN/GaN HEMTs[8] due to the suppression of the drain side gate edge electric field. However, conventional FP structures have some major drawbacks. (i) Limited improvement in suppressing drain side gate edge electric field strength. (ii) Limited improvement in breakdown voltage especially when the passivation layer is very thin, e.g., 150 nm. (iii) Breakdown location still happens either near the surface of the field plate edge or near the surface of the drain side gate edge. (iv) Field plates can introduce parasitics, which will affect device electrical characteristics.[9]

In this paper, we report on an HEMT structure with a localized Mg-doped layer under the 2-DEG channel. Comparing the HEMT with a conventional field plate (con. FP) with a double field plate (double FP), the proposed device exhibits suppression of the drain side gate edge electric field with a significant improvement of the breakdown voltage. The peak electric field shifts from the surface of the HEMT to bulk Mg-doped layer edge. The drain side gate edge electric field can be reduced by 5.5 times and 3 times compared with those of the HEMTs with optimized con. FP and double FP, respectively. The state-of-the-art process techniques that can lead to the realization of the pro-

†Corresponding author. E-mail: ngwt@vrg.utoronto.ca; xielyz@vrg.utoronto.ca

posed HEMT such as Mg implantation, selective epi growth, post-anneal activation as well as the damage removal have been investigated extensively.[10−13] The basic structure of its forward and reverse characteristics has also been reported in our previous work.[14] It has been demonstrated that the localized Mg-doped layer can allow a good trade-off between breakdown voltage and device on-resistance. Detailed electrical characteristics are verified using the APSYS simulator from Crosslight.[15]

2. Device structure and simulation model

Devices with a Mg-doped layer, con. FP and double FP are shown in Fig. 1, where $L_{\rm m}$ and $L_{\rm fp}$ are the length of the Mg-doped layer and the length of con. FP, respectively, $L_{\rm s}$ and $L_{\rm fg}$ are the source connected FP length and gate connected FP length for HEMT with double FP, respectively. The Mg layer is located 0.5-μm underneath the 2-DEG channel. All the HEMTs with Mg-doped layer, con. FP, and double FP have the same device physical dimensions as shown in Figs. 1(a)–1(c). The epitaxial layer structure consists of an unintentionally doped AlGaN barrier layer (33 nm)/C-doped insulating layer (3 μm). Al mole fraction in the AlGaN layer is 0.25. The thickness of the SiN passivation layer is 400 nm. A sheet carrier density of 1.1×10^{13} cm^{-2} caused by the piezoelectric and polarization dipole was modeled along the upper side of the AlGaN/GaN interface to determine the 2-DEG sheet carrier concentration. According to Chynoweth's[16] impact ionization model and a Monte Carlo simulation of the impact ionization in wurtzite GaN, the impact ionization model in our simulation is as shown below:

$$\alpha = \alpha_n^{\infty} \exp\left[-\left(\frac{Fcn}{F}\right)^{kn}\right], \qquad (1)$$

where α_n^{∞} and Fcn are the impact ionization rate and critical electric field for electrons, respectively. The same formula can be obtained for holes. Electron ionization rates and hole ionization rates can be calculated to be 2.6×10^8 cm^{-1} and 4.98×10^6 cm^{-1}, respectively. These values are used in the simulation. Traps with a maximum concentration of 1×10^{14} cm^{-3} and a relative energy level of 1.1 eV are also assigned to model the semi-insulating substrate to suppress parasitic substrate conduction. Electron mobility of 1800 cm$^2\cdot V^{-1}\cdot$S^{-1} was also modeled along the 2-DEG channel. Other device parameter values employed for simulation are shown in Table 1.

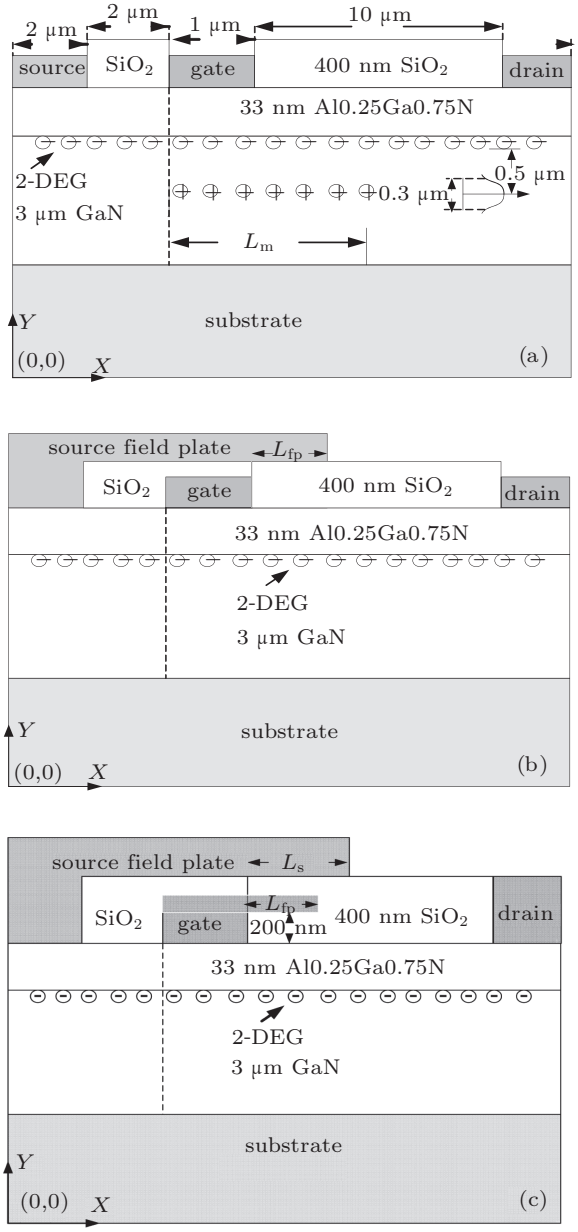

Fig. 1. Cross-sectional views of the proposed HEMT structure with (a) magnesium-doped layer, (b) conventional HEMT with a source-connected field plate, and (c) conventional HEMT with double field plates.

Table 1. Material parameters for simulation.

Parameters	AlGaN	GaN
Bandgap/eV	4.15	3.47
Electron mobility/cm$^2\cdot$V$^{-1}\cdot$S^{-1}	550	1100
Electron saturation velocity/cm$\cdot$s^{-1}	1.5×10^7	2.1×10^7
Dielectric constant	9.6	9.5
Critical electric field/(MV/cm)	5.5	3.0

3. Results and discussion

The simulated breakdown voltages each as a function of Mg layer concentration with different values of Mg-doped layer length L_m are plotted in Fig. 2(a). It can be observed that the optimum doping concentration for the Mg layer is 8×10^{17} cm^{-3} for different values of L_m. The breakdown voltage decreases dramatically when doping concentration is above or below 8×10^{17} cm^{-3} due to the charge imbalance. Figure 2(b) illustrates the simulation results of the breakdown voltage for HEMT with con. FP as a function of L_{fp}, and the breakdown voltage for the HEMT with 8×10^{17} cm^{-3} Mg-doped layer as a function of the doped layer length, L_m. From this figure, a maximum breakdown voltage of 900 V is obtained with $V_{gs} = -5$ V and $L_m = 1.5$ μm for the proposed HEMT. Continuing increase in L_m will cause a peak of the electric field on the drain side, lowering the breakdown voltage. While for HEMT with con. FP, breakdown voltage increases from 560 V without FP to 800 V with conventional L_{fp} length of ~ 3.5 μm. No further increase in breakdown voltage is observed after this point. Breakdown voltages each as a function of L_{fg} with different values of L_s are shown in Fig. 2(c).

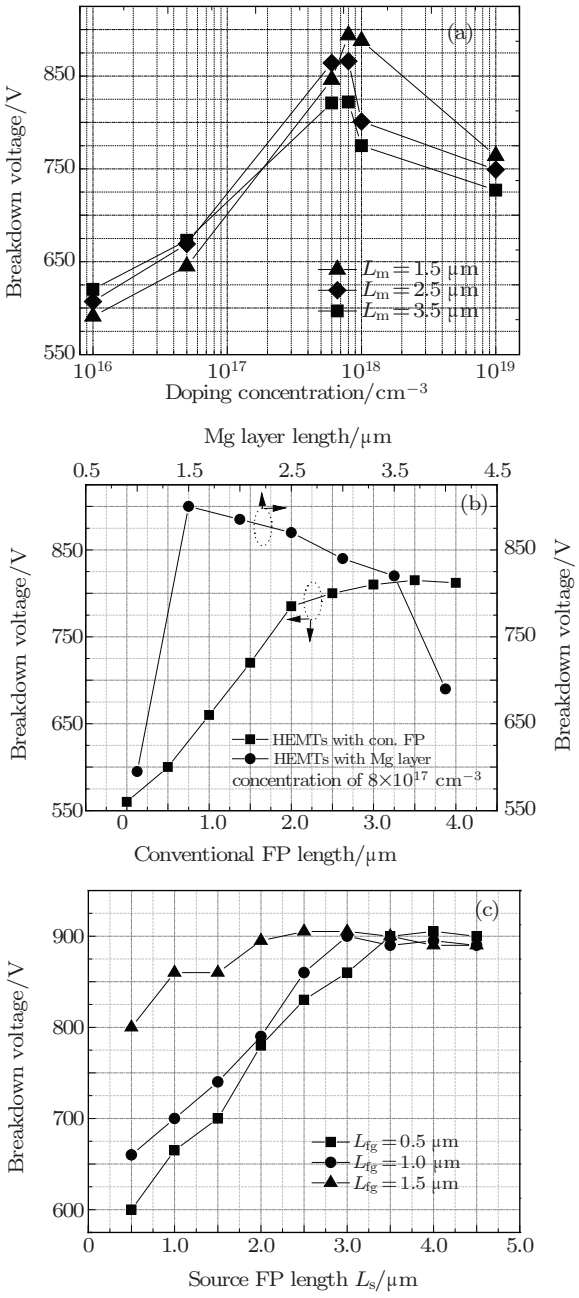

Fig. 2. (colour online) (a) Simulated breakdown voltages each as a function of Mg layer doping concentration with values of different L_m, (b) breakdown voltage for an HEMT with a Mg-doped layer as a function of L_m with an Mg doping concentration of 8×10^{17} cm^{-3} and breakdown voltage for HEMT with con. FP as a function of FP length L_{fp}. $V_{gs} = -5$ V and $T = 300$ K, and (c) breakdown voltages each as a function of L_s with different values of L_{fg} for the double FP structure.

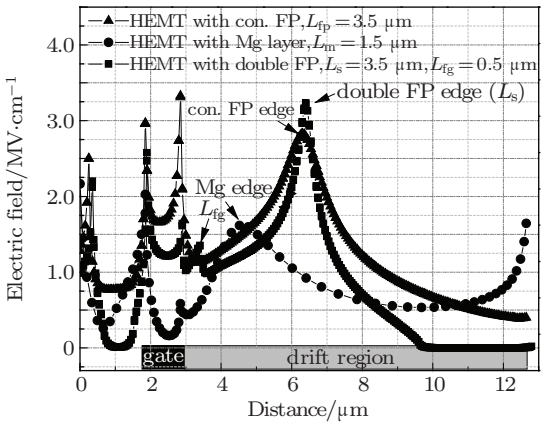

Fig. 3. Simulated surface electric distributions along the AlGaN/GaN interface for an HEMT with con. FP, double FP, and HEMT with Mg-doped layer at $V_{gs} = -5$ V, $L_m = 1.5$ μm, $L_{fp} = 3.5$ μm, $L_s = 3.5$ μm, and $L_{fg} = 0.5$ μm. Mg doping concentration = 8×10^{17} cm^{-3}, $T = 300$ K.

From Fig. 2(c), a breakdown voltage of 905 V at $L_s = 3.5$ μm and $L_{fg} = 0.5$ μm can be observed, where the breakdown voltage is comparable to that of the HEMT with Mg layer. In order to clarify this mechanism, the 2D surface electric field distribution is simulated to help the analysis. Figure 3 shows the simulated surface electric field distribution along AlGaN/GaN interface for an HEMT with a Mg-doped layer length of 1.5 μm, HEMT with a con. FP length of 3.5 μm and a double FP HEMT with $L_s = 3.5$ μm and $L_{fg} = 0.5$ μm. It can be observed that for an HEMT with con. FP, critical peak surface electric field is located near the drain side gate edge, where breakdown occurs. For the

HEMT with double FP, peak electric field shifts to the edge of source FP. Surface electric field strength for the HEMT with a Mg-doped layer is dramatically reduced as shown in Fig. 3. The drain side gate edge of surface electric field is reduced from 3.3 MV/cm for HEMT with con. FP and 1.7 MV/cm for the HEMT with double FP to 0.6 MV/cm for HEMT with Mg-doped layer, yielding a 5.5 times and 3 times the reduction of the gate edge surface electric field strength, respectively. Furthermore, from the three-dimensional (3D) electric field distribution shown in Fig. 4, the peak electric field of the HEMT with a Mg-doped layer shifts to the edge of the Mg-doped layer, which is far from the metal gate. This layer acts as a floating field plate to ensure a more evenly distributed surface electric field. While for the con. FP and double FP structures, two electric field peaks located in the 2-DEG channel (AlGaN/GaN interface) and the AlGaN/SiN interface are observed. Breakdown occurs in the 2-DEG channel near the gate edge for HEMT with con. FP and FP edge for the HEMT with a double FP.

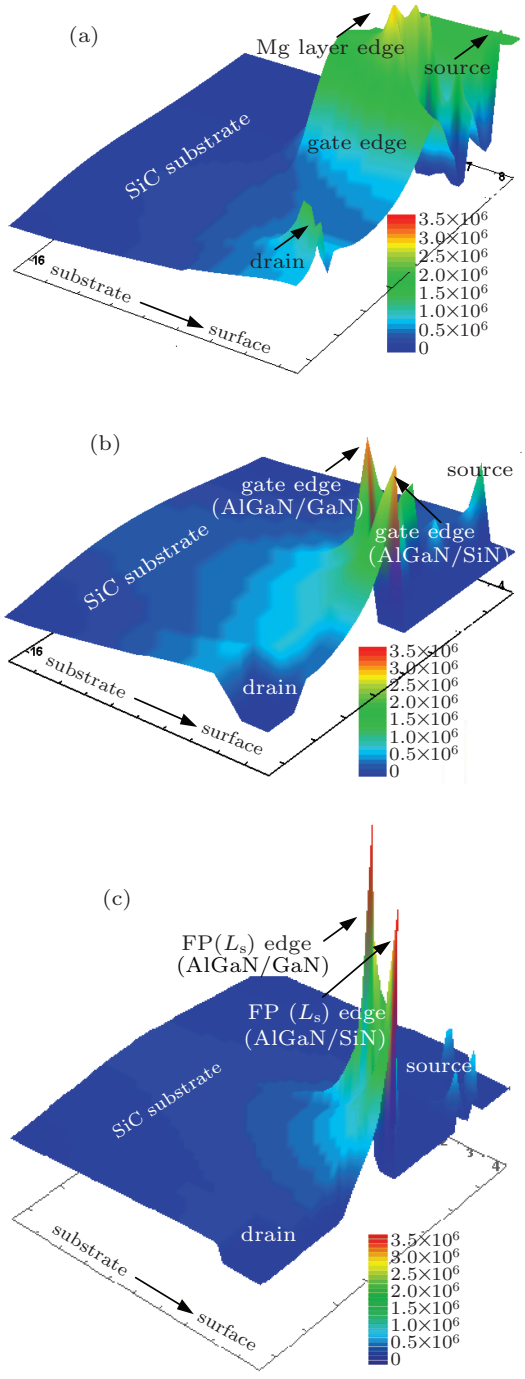

Fig. 4. (colour online) Simulated 3D electric field distributions in (a) HEMT with Mg-doped layer, magnesium doping concentration = 8×10^{17} cm^{-3}, $L_m = 1.5$ μm, (b) HEMT with con. FP at $V_{gs} = -5$ V, $L_{fp} = 3.5$ μm, and $T = 300$ K, and (c) HEMT with double FP at $V_{gs} = -5$V, $L_s = 3.5$ μm, and $L_{fg} = 0.5$ μm, $T = 300$ K.

The gate to drain leakage current is also simulated and analysed in Fig. 5. The drain to gate leakage current for the proposed device at $V_{gs} = -5$ V and $V_{ds} = 400$ V is 16 nA/mm to 19 nA/mm, while that for the device with con. FP is 120 nA/mm. The gate leakage current is reduced by more than one order of magnitude. This is attributed to the reduction of the electric field strength at the gate edge compared with that of the conventional structure.

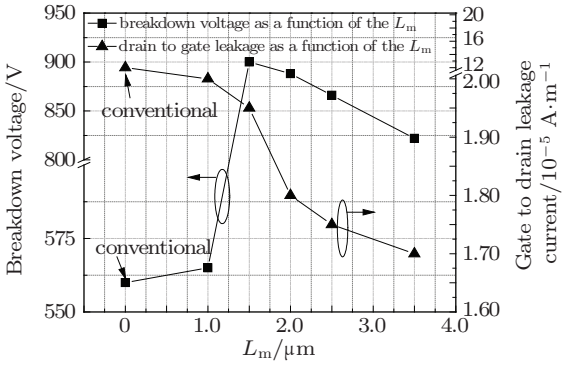

Fig. 5. Simulated breakdown voltage and the drain to gate leakage current ($V_{ds} = 400$ V) each as a function of L_m, at $V_{gs} = -5$ V, Mg doping concentration = 8×10^{17} cm^{-3}, and $T = 300$ K.

Figure 6 shows the transfer and transconductance characteristics for the con. HEMT, HEMTs, respectively, with source connected FP and double FP. The threshold voltage is −4.5 V for conventional HEMT, while for HEMT with double FP, the threshold voltage exhibits −3.7 V. This is due to the lowest potential of the metal FP that can affect the 2-DEG channel.[9] The peak transconductance for the HEMT with double FP is also reduced from 540 ms/mm for con. HEMT to around 480 ms/mm for double FP. The HEMT with Mg-doped layer shows a comparable g_m

and a little degradation in $V_{\rm th}$ due to the interaction between the channel and Mg layer.

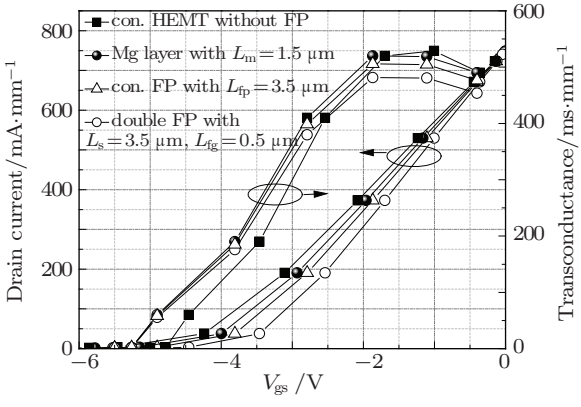

Fig. 6. Simulated transfer and transconductance characteristics for the con. HEMT, HEMT with Mg layer, HEMT with con. FP, HEMT with double FP, where $L_{\rm m} = 1.5$ μm, $L_{\rm fp} = 3.5$ μm, $L_{\rm s} = 3.5$ μm, $L_{\rm fg} = 0.5$ μm, and $T = 300$ K.

The simulations of cut-off frequency are as illustrated in Fig. 7. With $V_{\rm ds} = 20$ V and $V_{\rm gs} = -2$ V, the cut-off frequencies for the con. HEMT, the HEMT with Mg-doped layer, the HEMT with con. FP, and the HEMT with double FP are 38 GHz, 32.5 GHz, 27 GHz, and 25 GHz, respectively.

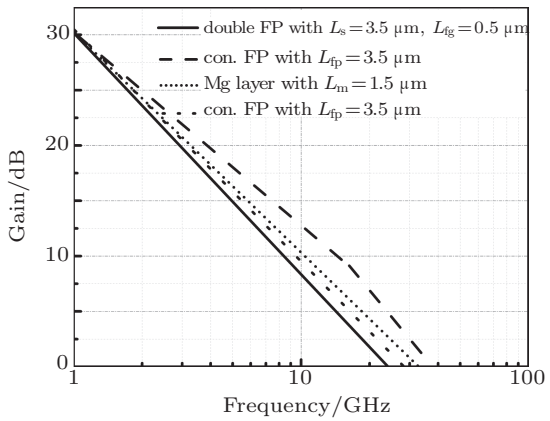

Fig. 7. Small signal simulations for the con. HEMT, HEMT with Mg layer, HEMT with con. FP, HEMT with double FP, where $L_{\rm m} = 1.5$ μm, $L_{\rm fp} = 3.5$ μm, $L_{\rm s} = 3.5$ μm, and $L_{\rm fg} = 0.5$ μm, $V_{\rm gs} = -2$ V, $V_{\rm ds} = 20$ V, and $T = 300$ K.

The degradations of $f_{\rm T}$ for the HEMT with con. FP and the HEMT with double FP are due to the overlap between source metal FP and gate metal FP that can induce parasitic capacitance.

4. Conclusion

In this paper, we proposed a high voltage AlGaN/GaN HEMT with a localized Mg-doped layer. The Mg layer acts as a field shaping layer, thereby successfully suppressing the drain side gate electric field strength. The drain side gate edge peak electric field of the HEMT with Mg-doped layer is reduced by 5.5 times and 3 times compared with those of the HEMT with con. FP and the HEMT with double FP, respectively. The proposed Mg-doped HEMT also exhibits less degradations in $g_{\rm m}$, $V_{\rm th}$, and $f_{\rm T}$ with one order of magnitude improvement in the gate leakage current. This reducing surface electric field technique is very promising for use in wide band gap based power switching applications.

References

[1] Ibbetson J P, Fini P T, Ness K D, DenBaars S P, Speck J S and Mishra U K 2000 *Appl. Phys. Lett.* **77** 250

[2] Nanjo T, Takeuchi M, Suita M, Oishi T, Abe Y, Tokuda Y and Aoyagi Y 2008 *Appl. Phys. Lett.* **92** 263

[3] Zhang J F, Mao W, Zhang J C and Hao Y 2008 *Chin. Phys.* B **17** 689

[4] Guo B Z, Gong N and Yu F Q 2008 *Chin. Phys.* B **17** 290

[5] Hong S K, Shim K H and Yang J W 2008 *Electronic Lett.* **44** 1091

[6] Xu C, Wang J, Chen H, Xu F, Dong Z, Hao Y and Wen C P. 2007 *IEEE Electron Dev. Lett.* **28** 942

[7] Choi Y H, Lim J Y, Cho K H, Kim Y S and Han M K 2009 *Mater. Sci. Forum.* **615** 971

[8] Ando Y, Okamoto Y, Miyamoto H, Nakayama T, Inoue T and Kuzuhara M 2003 *IEEE Electron Dev. Lett.* **24** 289

[9] Saito W, Takada Y, Kuraguchi M, Tsuda K, Omura I, Ogura T and Ohashi H 2003 *IEEE Electron Dev. Lett.* **50** 2528

[10] Hwang J D and Yang G H 2007 *Appl. Surf. Sci.* **253** 4694

[11] Whelan S, Kelly M J, Yan J and Fortunato G 2005 *Phys. Status Solidi* **2** 2472

[12] Cao X A, Wilson R G, Zolper J C, Pearton J S, Han J, Shul R J, Rieger D J, Singh R K, Fu M and Scarvepalli V 1999 *J. Electron. Mater.* **28** 261

[13] Li S Q, Wang L, Han Y J, Luo Y, Deng H Q, Qiu J S and Zhang J 2011 *Acta Phys. Sin.* **60** 098107 (in Chinese)

[14] Xie G, Zhang B, Fu F Y and Ng W T 2010 ISPSD, Hiroshima, Japan

[15] www.crosslight.com, user's manual.

[16] Chynoweth A G 1958 *Phys. Rev.* **109** 1537